Heterogeneous & Homogeneous & Bio- & Nano-

CHEMCATCHEM

CATALYSIS

Accepted Article

Title: Aluminum containing dendrimeric silica nanoparticles as promising metallocene catalyst supports for ethylene polymerization

Authors: Duarte M. Cecílio, Auguste Fernandes, João Paulo Lourenço, and M. Rosário Ribeiro

To be cited as: *ChemCatChem* 10.1002/cctc.201800534

Link to VoR: http://dx.doi.org/10.1002/cctc.201800534

A Journal of

ChemPubSoc Europe

WILEY-VCH

www.chemcatchem.org

Aluminum containing dendrimeric silica nanoparticles as promising metallocene catalyst supports for ethylene polymerization

Duarte M. Cecílio[b], Auguste Fernandes[b], João Paulo Lourenço*[a,b] and M. Rosário Ribeiro*[b]

Abstract: Several aluminum containing dendrimeric silica nanospheres, DSAl materials, were prepared using different synthesis and post-synthetic procedures. These materials were used for the immobilization of Cp_2ZrCl_2 via direct impregnation. The support materials were rigorously characterized by TEM, N_2 adsorption, FTIR (using pyridine as probe molecule) and SS-NMR in order to assess their morphological, textural and surface acidic properties. Supported catalysts were tested in ethylene homopolymerization using methylaluminoxane (MAO) as co-catalyst and scavenger. The relationships between the types and strength of acid sites, as well as the textural and morphological parameters of DSAl materials with the behavior of catalytic systems is explored in this work. The results analyzed in this paper confirm the importance that support surface acidity plays in the formation of the active species for ethylene polymerization and in its activity without neglecting the contribution of support textural properties as well.

Introduction

Most industrial olefin polymerization processes, namely slurry and gas phase, require solid catalysts owing to their ability to control polymer morphology and to prevent reactor-fouling problems. Catalyst support materials in olefin polymerization present a crucial influence in both catalytic activity and final particle morphology, depending on their specific structure. The size of the support particles, base morphology, textural parameters such as surface area, pore volume and porosity will directly influence the properties of the resulting polymer particle. For industrial purpose, catalysts are generally supported on silica, which enables the versatility and simple processing of the catalyst. Several types of porous silica have been recently explored for the control of particle morphology and reaction yield improvement. Examples include the mesoporous nanosilicas MCM-41 and SBA-15, amongst other various unique types of silica[1,2].

Hierarchical porous materials present a wide range of potential applications in the fields of energy conversion/storage, catalysis, separation and biomedical applications[3]. Particularly in the field of catalytic applications, porous nanomaterials have seen an increase in interest due to their attractive textural parameters. An essential feature of this type of materials is that many of them do not show a very high reactive surface and are catalytically inert, as is the case of silica[4]. This creates an added difficulty in both direct catalysis or in the adsorption of catalyst molecules. One possibility to address this limitation is the incorporation of heteroatoms in the matrix, either by direct synthesis or by post-synthesis grafting procedures, aiming to introduce acidity into the support surface[5,6,15,7–14]. One of the most common heteroatoms is aluminum, although some transition metals can also be employed. The amount of heteroatoms and their chemical environment will determine the surface acidity of the support through the distribution of Lewis and Brønsted acid sites. The importance of the acidic surface properties of supports in the activation of metallocene catalysts and their subsequent performance in polymerization has been discussed in the literature[2,5,16–22].

There are different methods for the immobilization of metallocene catalysts on the surface of a mesoporous silica or aluminosilicate. Two of the most widely used include: (i) the direct impregnation of the transition metal complex onto the support surface and (ii) a pre-treatment of the support surface with a co-catalyst (usually MAO) prior to the contact with the complex. However, when considering modified aluminosilicates it was found that a pre-treatment of the surface with MAO extensively dilutes the effect of surface acidity on polymerization activity[7]. In the case of direct impregnation, Rahiala *et al.*[23] analysed the behaviour of Al-MCM-41 in ethylene polymerization when compared to purely siliceous MCM-41 and commercial Grace silica, reaching the conclusion that the modification of the siliceous framework with aluminium improves polymerization activity although the high surface area of MCM-41 could not be proven to have a large effect in activity. Campos *et al.*[7] confirmed that the presence of aluminium in the framework of a mesoporous Al-MCM-41 improves not only the catalyst activity in ethylene homopolymerization but also improves the immobilization of the catalyst on the support surface, leading to higher metal loadings compared to Si-MCM-41.

[a] Dr. J. P. Lourenço
Centro de Investigação em Química do Algarve (CIQA),
Departamento de Química e Farmácia,
Faculdade de Ciências e Tecnologia,
Universidade do Algarve, Campus de Gambelas, 8005-139 Faro, Portugal
E-mail: jlouren@ualg.pt

[b] MSc D. M. Cecílio, Dr. A. Fernandes, Dr. J. P. Lourenço, Dr. M. R. Ribeiro
Centro de Química Estrutural (CQE), Departamento de Engenharia Química,
Instituto Superior Técnico, Universidade de Lisboa
Av. Rovisco Pais 1, 1049-001 Lisboa, Portugal

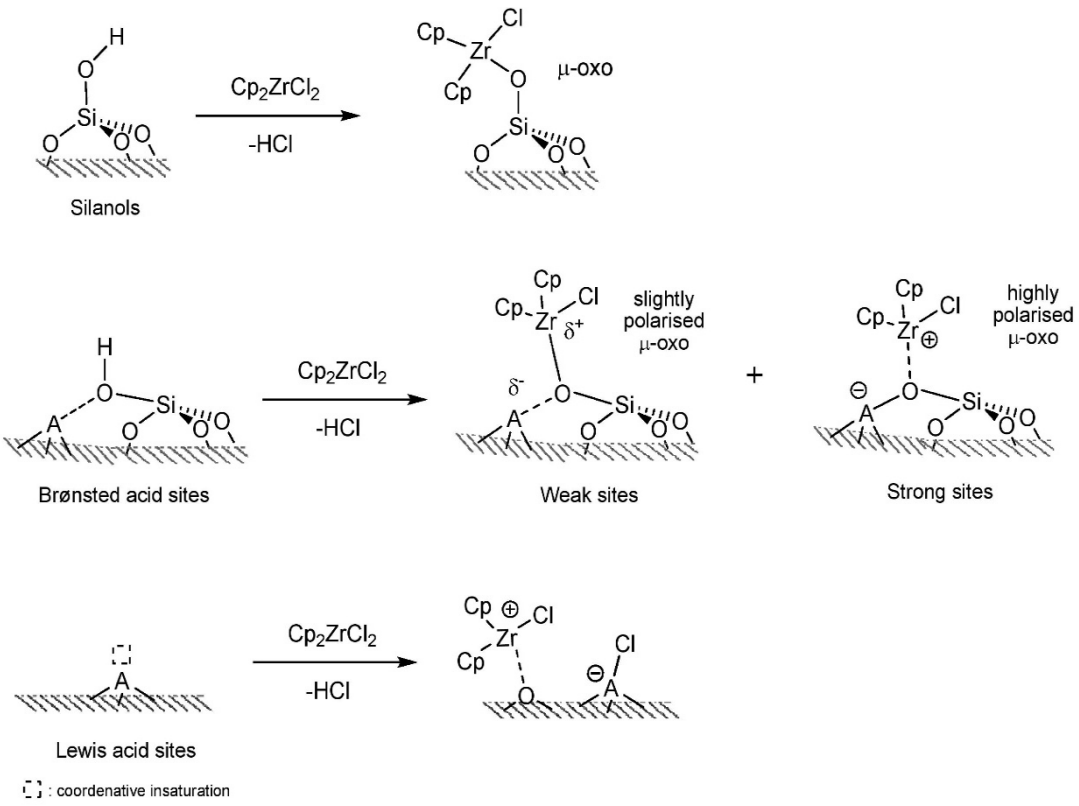

Scheme 1. Models for the interactions of metallocene Cp_2ZrCl_2 with species present in acidic silicate surfaces (A: acidic element). Reprinted with permission from Campos et al,[5] Copyright(2009) with permission from Elsevier.

In recent years, Polshettiwar *et al.*[24] reported the discovery of a novel kind of hierarchical mesoporous silica consisting of nanospheres with radial growth of dendrimeric fibers (KCC-1) that reportedly presents both high accessibility and high values of surface area. This dendrimeric silica will be henceforth referred to as DS. More recently, Bayal *et al.*[25] reported a tunable synthesis method for DS that allows for control of particle size and textural parameters, while Ernawati *et al.*[26] reported a different TMOS-based tunable synthesis method and studied the effect of synthesis conditions on the morphology of the resulting fibrous silica nanospheres. Concerning the catalytic applications, Lee *et al.*[1] studied purely siliceous DS as support for metallocene catalysts on ethylene polymerization. In this case the authors performed a methylaluminoxane (MAO) pre-treatment before the catalyst loading and studied the morphology of the resulting polymer. The results have shown that the large surface area and open pore entrances offer minimal constraints to the catalyst diffusion and immobilization and play a central role in the performance of the catalytic system.

Published works on the modification of DS aiming at the introduction of acidic properties have been scarce, however a few studies have shown its feasibility. Choi *et al.*[4] reported a facile two-step direct synthesis approach to preparing tuneable acid nano-catalysts by modifying a DS-like material with aluminum and phosphorous, and afterward compared with Al-MCM-41 and HZSM-5 samples in the cracking of 1,3,5-triisopropylbenzene and hydrolysis of sucrose. In another study, Yang *et al.*[27] reported the synthesis of core-shell magnetic particles containing a magnetic core and an outer shell composed of DS-like silica modified with Al through a post-synthesis impregnation method. Shahangi *et al.*[28] reported the synthesis of DS-Al via a one-step direct synthesis method and its further use as an acid catalyst for the dehydration of fructose and sucrose. Afzal *et al.*[29] reported a one-pot synthesis of manganese incorporated DS like materials for catalytic ozonation. Although acidic DS has been tested in diferent catalytic reactions, to the best of our knowledge no study has been reported on the use of acidic DS in olefin polymerization.

Several authors have studied the effect of the surface chemistry of the support in the direct immobilization of metallocene catalysts and on the generated species, their reactivity and corresponding polymerization activity[30–35]. The importance of surface acidic properties in mesoporous silicas, i.e., MCM-41, to improve support performance in metallocene catalyst immobilization and overall catalytic performance in ethylene polymerization was also demonstrated in previous works reported by our group[5–7]. The nature and the strength of the surface acid sites play a crucial role in the catalytic system,

influencing the interaction of the metallocene complex with the support. The formation of active cationic, "cationic-like" or polarized species, in addition to other inactive or barely active species containing μ-oxo or Zr–O–Si structures is dependent on the type of acid site and will influence the final catalytic performance. A schematic representation of the interaction of zirconocene dichloride (Cp_2ZrCl_2) with supports containing different acid sites, that was previously proposed[5], is shown in scheme 1. The species illustrated are not active by themselves but may be activated in presence of MAO, where the cationic or strongly polarized species (originated on Lewis or strong Brønsted sites) are more prone to be converted to active species than the slightly polarized μ-oxo or neutral metallocene complexes.

In the present work, we present the synthesis of Al-containing DS type materials (DSAl) via two distinct direct synthesis methods and a post-synthesis incipient wetness impregnation method, intending to compare the influence of the method on the properties of the resulting supports. The samples are characterized concerning morphology, textural properties, chemical composition and surface acidic properties, which are then correlated with their catalytic performance in ethylene homopolymerization.

Results and Discussion

The first step in this work consisted in the synthesis and characterization of a purely siliceous DS batch to serve as reference for the modified DSAl samples. The following TEM micrographs present the morphology results for this reference batch.

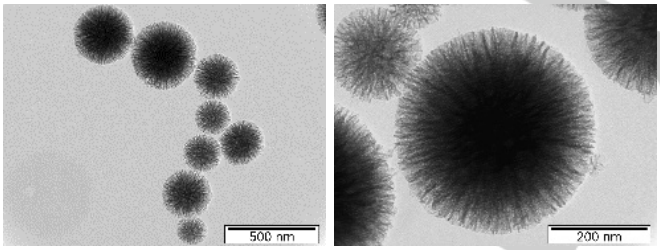

Figure 1. TEM micrographs of the reference DS batch.

The TEM micrographs presented in figure 1 confirm the expected spherical dendrimeric morphology. The sample presents a broad particle size distribution with particle diameter ranging from 100 nm to 600 nm. However, the average particle size is similar to that reported by Polshettiwar *et al.*[24]. Figures 2 and 3 present both the nitrogen sorption isotherm and the pore size distribution that result from the sorption measurements. DS reference material presents a surface area of about 370 m^2/g and a total pore volume of 0.7 cm^3/g. Application of BJH method reveals a bimodal pore size distribution with two populations with maxima at approximately 3 and 20 nm.

The following step of the work consisted in the modification of DS nanospheres with aluminum, in order to introduce acidity onto the support. To highlight the effect of the synthesis method on the textural and acidic properties of the material, three samples were prepared with a similar Si/Al ratio, using different Al incorporation methods (post-synthesis impregnation and direct method, with one or two synthesis steps). To extend the study on the influence of the synthesis conditions, a second sample with a lower Si/Al was also prepared, using the two-step direct method. Although the samples prepared show differences concerning the textural and acidic properties as described below, it is clear that all the methods tested allow to prepare Al-containing DS type materials with a good degree of control over the amount of aluminum incorporated. A good agreement between the Si/Al ratios in the synthetic gel and in final sample is observed, suggesting that the presence of Al does not significantly change the kinetics involved in the formation of the crystalline phase.

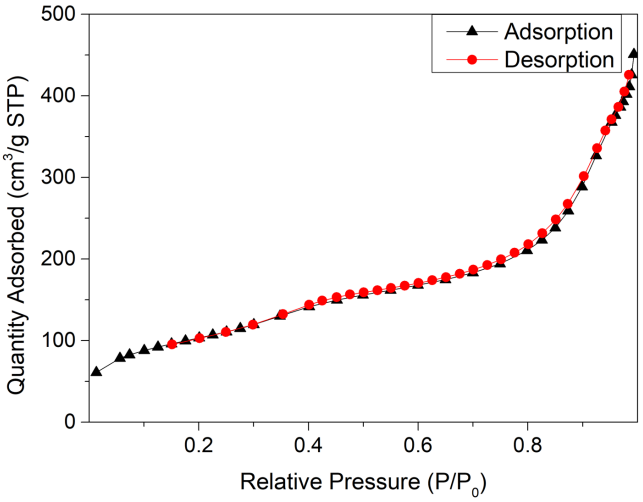

Figure 2. Nitrogen sorption isotherm for the DS reference batch.

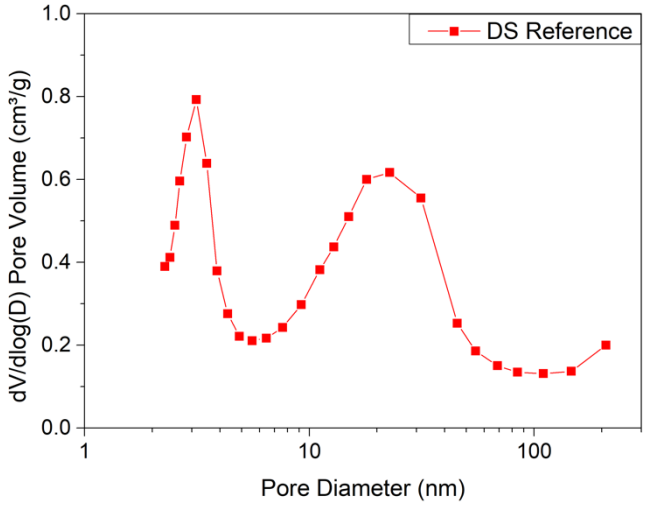

Figure 3. BJH Pore Size Distribution for the DS reference batch calculated from the adsorption branch.

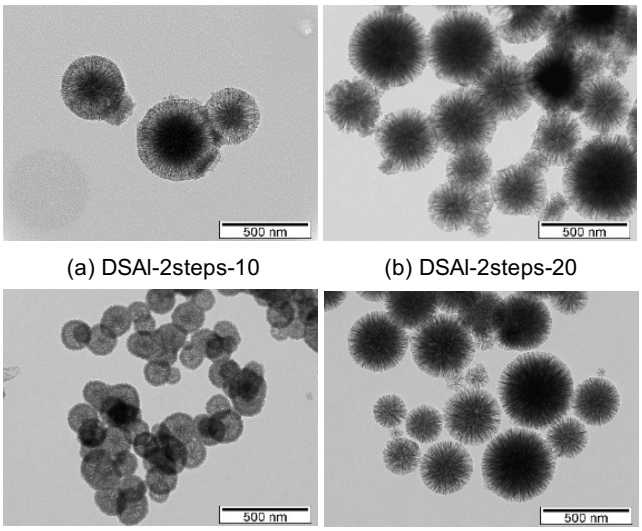

(a) DSAl-2steps-10 (b) DSAl-2steps-20

(c) DSAl-1step-20 (d) IWI-DSAl-20

Figure 4. TEM micrographs of the DSAl samples.

The TEM micrographs presented in figure 4 show slight differences in morphology between the various samples, although the spherical dendrimeric morphology is generally retained with the addition of aluminum. Sample DSAl-2steps-10 shows a slightly more open morphology when compared to the purely siliceous DS (figure 1).

Comparing synthesis methods for a Si/Al ratio of 20, sample IWI-DSAl-20 prepared by incipient wetness impregnation shows a morphology expectedly similar to the DS reference batch (figure 1), while sample DSAl-1step-20 prepared by one-step direct synthesis presents two main differences: the first is the smaller size of the nanospheres when compared to the other two methods and the second is the slightly distorted shape of some particles, oblong rather than spherical.

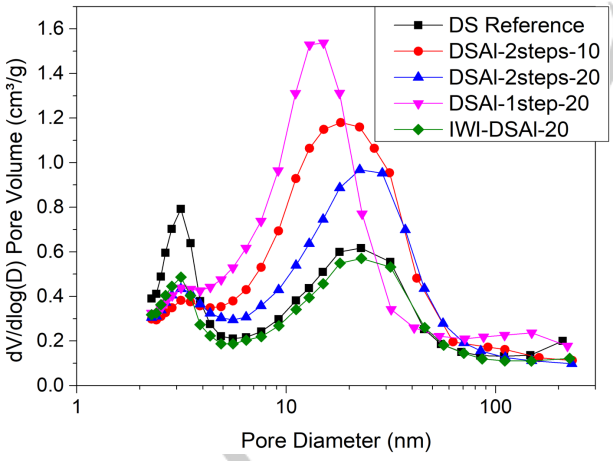

Figure 5. Pore size distribution for the analyzed samples (BJH method, adsorption branch).

Regarding the textural properties of the DSAl supports, table 1 shows that both the method and the synthesis conditions influence the surface area and pore volume, albeit with different magnitudes. The two samples synthesized via two-step direct synthesis method show some variation of the textural parameters. When comparing the different synthesis methods for a desired Si/Al ratio of 20, the variations are clearer. The one-step direct synthesis method yields the highest surface area and pore volume values, while incipient wetness impregnation yields the lowest ones due to the textural properties of the already existing DS sample and the deposition of aluminum on the pores surface of the material that may cause some pore blockage.

The pore size distribution data presented in figure 5 show that the bimodal distribution observed with DS nanospheres is retained with aluminum introduction, although some differences are observed between samples. It is evident from the data that the incorporation of aluminum gives rise to a decrease of the population of pores with the smallest diameter when compared with the population of pores with large diameter.

Comparing the different synthesis methods, the one-step direct synthesis approach yields significantly lower average pore size due to the smaller spheres formed during this process, as corroborated by the TEM micrograph shown in figure 4. Sample IWI-DSAl-20 prepared by incipient wetness impregnation shows an expected pore size distribution, similar to the DS reference but presenting lower pore volume due to the deposition of aluminum inside the already existing pores, mostly in the small pore population (figure 5).

Quantitative assessment of the acidic properties of the different supports was done by FT-IR spectroscopy with pyridine as probe molecule. Using pyridine is advantageous since it allows to differentiate between Lewis and Brønsted acid sites. Bands at 1457 and 1621 cm^{-1}, attributed to Lewis acid centres, are observed together with bands at 1545 and 1640 cm^{-1}, usually assigned to Brønsted acid sites[5]. The band at 1491 cm^{-1} appears due to a simultaneous contribution of both types of acid sites. Figure 6 presents IR spectra obtained for DSAl materials, only in the range relevant for the quantification of acidity, being the quantitative acidity measurements shown in table 1. It is worth noting that Lewis acidity at 150ºC varies just from 58 to 70 µmol/g while variation in Brønsted acidity is more significant, from 20 to 46 µmol/g. When compared with other types of mesoporous silica prepared in our research group[36], the results suggest that lower Si/Al ratios are needed for DSAl to achieve a similar number of accessible acid sites. For this reason, rather low Si/Al ratios were selected when synthesizing the different samples.

Table 1. Characterization of the synthesized samples regarding Si/Al ratio, textural properties and acidic properties.

Sample	Si/Al Synthesis gel	Si/Al Final solid [a]	S_{BET} (m^2/g)[b]	V_P (cm^3/g)[c]	Lewis Acidity[d]		Brønsted Acidity[d]		Average diameter (nm)[e]	
					150ºC	300ºC	150ºC	300ºC	Small pores	Large pores
DS	-	-	372	0.70	-	-	-	-	3	23
DSAl-2steps-10	10	8	396	1.02	67	42	32	0	3	18
DSAl-2steps-20	20	18	355	0.86	58	43	24	0	3	22
DSAl-1step-20	20	19	478	1.10	63	43	20	0	3	15
IWI-DSAl-20	20	22	298	0.60	70	8	46	0	3	23

[a]Determined by bulk chemical analysis.
[b]S_{BET} determined in the range of $0.05 < p/p^0 < 0.3$
[c]V_P determined for $(p/p^0) = 0.995$
[d] µmol/g
[e] Determined from the BJH method on the adsorption branch

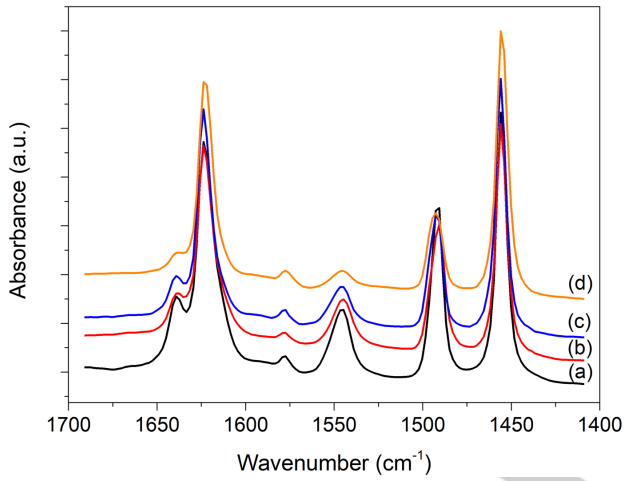

Figure 6. FT-IR spectra of the samples after pyridine desorption at 150ºC: (a) DSAl-2steps-10, (b) DSAl-2steps-20, (c) DSAl-1step-20, (d) IWI-DSAl-20

Moreover, by lowering the Si/Al ratio in the synthesis preparation from 20 to 10 the Lewis acidity increases from 58 to 67 µmol/g while the Brønsted acidity increases from 24 to 32 µmol/g. Taking into account that the amount of aluminum introduced in the synthesis gel has doubled and the incorporation is confirmed through the decrease of the experimental Si/Al ratio from 18 to 8, this suggests that most of the incorporated aluminum does not contribute to acid sites creation. This may be due either to aluminum not being accessible or to an inappropriate chemical environment.

By comparing the acidity values calculated at 150ºC and 300ºC, it is possible to assess the strength of the acid sites. Results in table 1 show that for the samples synthesized by direct synthesis, most Lewis acid sites are strong. Additionally, all direct synthesis samples present approximately the same Lewis acidity at 300ºC. On the other hand, Brønsted acidity is weak, since no sample presents any Brønsted acid sites at 300ºC.

Comparing the different synthesis methods, samples prepared by either one-step or two-step direct synthesis present similar surface acidity while sample IWI-DSAl-20 prepared by incipient wetness impregnation presents relevant differences. The sample presents the highest acidity at 150ºC, in terms of both Lewis and Brønsted acidity but most of the acid sites are weaker than those presented by samples prepared by direct synthesis, since only 8 µmol/g of Lewis acid sites are available at 300ºC.

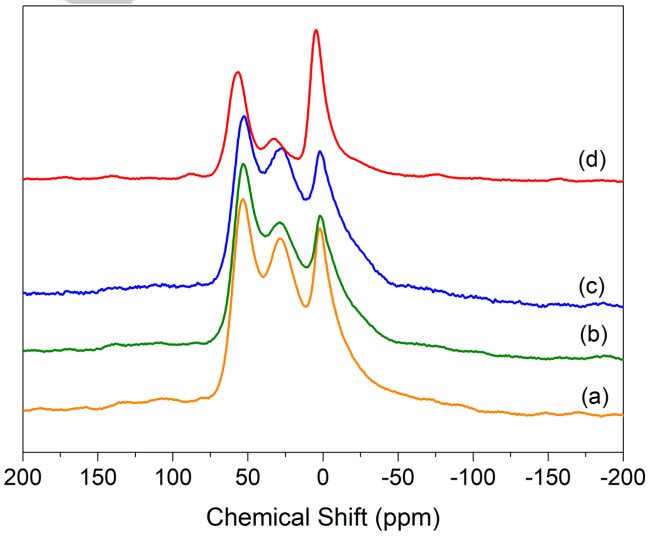

Figure 7. Solid-state ^{27}Al-NMR spectra for the DSAl samples: (a) DSAl-2steps-10, (b) DSAl-2steps-20, (c) DSAl-1step-20, (d) IWI-DSAl-20

Another important aspect to consider is the nature and distribution of the Al species on the support surface. Figure 7 shows the solid state ^{27}Al-NMR and three distinct peaks are visible for each sample. The peaks at 50 ppm and approximately 0 ppm correspond to tetrahedral and octahedral aluminum species, respectively. The occurrence of an intermediate peak at approximately 25 ppm and its nature is unclear. It might correspond to a penta-coordinated aluminum species or a distortion of the environments assigned to one of the other

peaks. The results appear to agree with the work done by other research groups, apart from the intensity of this intermediate peak.

Choi *et al.*[4] found the appearance of a small intermediate peak with the same chemical shift for samples with low Si/Al ratios (Si/Al=15), with the peak disappearing as the Al content decreases. Yang *et al.*[27] synthesized core-shell particles with a dendritic aluminosilicate shell and a Si/Al ratio of 14. The solid-state ^{27}Al-NMR spectrum presented in their work also contained a small peak at a chemical shift of approximately 25. However, the peak in this case appeared to be a distortion of the tetrahedral aluminum environment. It is worth noting that despite all the samples present the same types of aluminum species, the relative proportion of those species varies significantly when comparing samples prepared by direct synthesis (1step or 2steps) with the one obtained by incipient wetness impregnation.

Table 2. Catalysts prepared and activities obtained in ethylene polymerization, for Al/Zr=1500.

Support	Zr content in support (μmol/g)	Activity[c] ($kg_{PE}/mol_{Zr}h$)
Si-MCM41[a]	13[b]	830
Al-MCM41-16[a]	50	1610
DS Reference	12[b]	1300
DSAl-2steps-10	20	1000
DSAl-2steps-20	20	2300
DSAl-1step-20	20	2490
IWI-DSAl-20	20	1040

[a]data from J. M. Campos[36]
[b]maximum loading supported by the purely siliceous material
[c]average value obtained from ethylene consumption

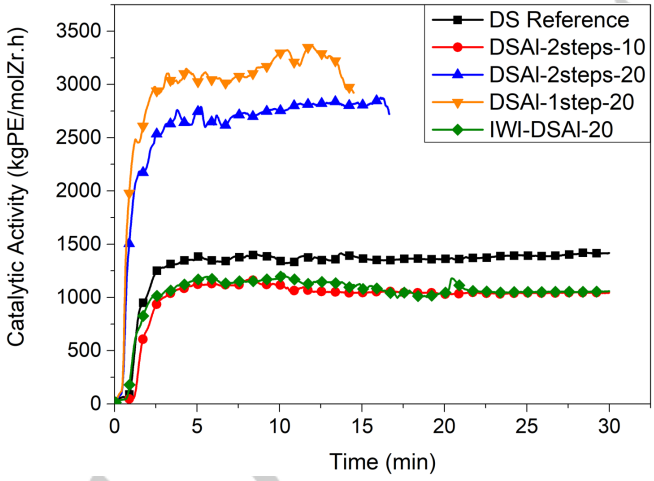

Figure 8. Kinetic profiles for the analyzed DSAl samples.

Preliminary polymerization tests were performed with the different supported catalytic systems derived from the various DSAl materials, in order to learn how this new kind of dendrimer shaped silica nanospheres behave and how its structural features may influence ethylene polymerization. Table 2 presents the Zr loading for each support and the corresponding polymerization activities. The kinetic profiles observed during ethylene polymerization are presented in figure 8. For comparison purposes, data regarding *in situ* ethylene polymerization using Si-MCM-41 and Al-MCM-41 supported zirconocene catalysts (the latter with a Si/Al ratio of 16) are also shown in table 2. The results indicate a clear improvement in catalytic activity of both DS and DSAl supported catalysts over their Si-MCM-41 and Al-MCM-41 counterparts. Results in table 2 and figure 8 also show that, when comparing the three different synthesis methods for the same Si/Al ratio of 20, a significant difference is observed between the samples prepared by direct synthesis and the sample prepared by post-synthesis modification. Samples DSAl-1step-20 and DSAl-2steps-20 show clear improvements over the reference DS batch, with approximately twice the average activity while sample IWI-DSAl-20 presents a much lower activity, slightly lower than the non-acidic DS reference.

It was previously reported that the presence of an acidic element (for example M = Al, Ga, Zn, Ti) in the framework of a silica material can be used to enhance the performance of a supported catalyst, although optimal chemical compositions and acidic features must be found in order to achieve high polymerization activities. Moreover, these chemical effects will only be clearly visible if other effects of different nature such as, changes in textural properties or diffusion resistances are not operating simultaneously. This way a complex balance of several effects may be operating and must be taken in account when analyzing the polymerization behavior.

It appears from the data in tables 1 and 2 that both DS silica samples showing the highest activities were prepared by the direct synthesis route (1- or 2-steps) and exhibit analogous acidic properties, both in terms of Lewis and Brønsted sites. However, they show different textural features, with a higher surface area and pore volume being observed for the sample prepared by the 1-step route, which is also leading to the most active catalytic system. On the other hand, sample IWI-DSAl-20, show a much lower surface area and pore volume as well as distinct acidic properties when compared to the above-mentioned DSAl 1- and 2-steps samples. It is also worth noting that the accessible Lewis acid sites present in sample IWI-DSAl-20 are mostly weak when compared to the other samples. Moreover, a strong increase in the number of weak Brønsted acid sites may be observed as well. Strong Lewis acidity is – within a certain range – beneficial towards metallocene immobilization and catalytic activity while weak Brønsted sites, may lead to the formation of μ-oxo species less prone to activation and therefore may cause detrimental effects[5,36]. The use of IWI-DSAl-20 as support gives rise not only to the lowest polymerization activity within the (Si/Al=20) series but also to a slightly lower activity than the DS reference. Comparing the pore size distribution of the DSAl support prepared by incipient

wetness impregnation (table 1 and figure 5) with purely silica DS reference it may be concluded that the decrease in pore volume and surface area comes essentially from the deposition of aluminum in the pore surface of the small pore population. This indicates that the aluminum is incorporated mostly inside these pores and the acid sites may not be evenly distributed. This might create an accessibility issue inside the porous structure for the bulkier catalyst and co-catalyst molecules that remain mostly in the bigger pores and external surface where there are fewer acid sites.

The behavior of sample DSAl-2steps-10 is more difficult to explain. Results in table 1 show higher acidity and higher surface area than sample DSAl-2steps-20. However, considering the aforementioned small variation of surface acidity (with higher aluminum content, i.e. lower Si/Al ratio), this may indicate an accessibility issue to the existing acid sites. Furthermore, it is worth noting that in table 1 and figure 5 it is observed that sample DSAl-2steps-10 has narrower pores than sample DSAl-2steps-20. This confinement effect can present a significant role in polymerization due to the importance of pore diameter in the immobilization of the zirconocene catalyst molecules and later access of the MAO co-catalyst to the catalyst present inside the pores.

Figures 9 and 10 plot the average activity versus the Lewis and Brønsted acidity of all the analysed samples.

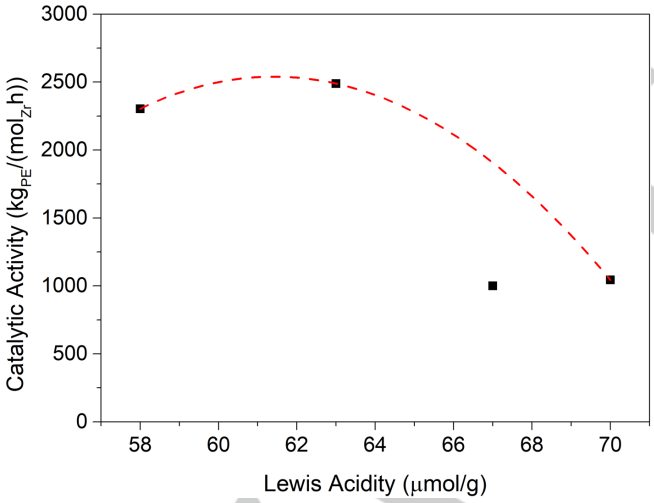

Figure 9. Polymerization activities for Al/Zr=1500 plotted as a function of Lewis acidity of the supports.

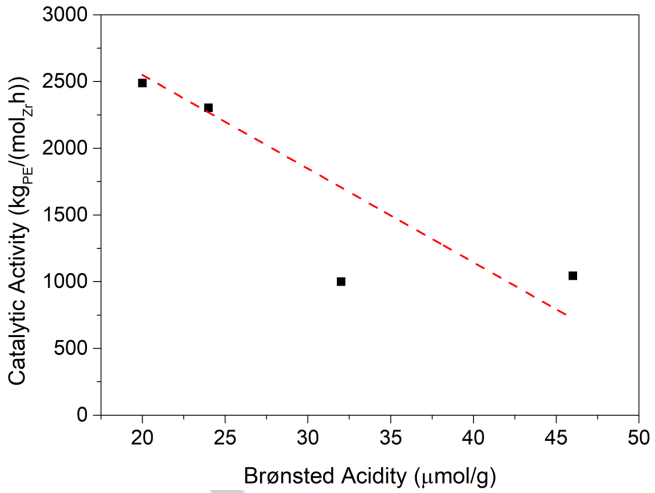

Figure 10. Polymerization activities for Al/Zr=1500 plotted as a function of Brønsted acidity of the supports.

Figure 9 presents a trend that suggests an optimum Lewis acidity for polymerization activity. It seems that introduction of Al in pure DS materials improves the catalytic activity, but an optimal support composition and corresponding surface acidity must be achieved. However, the Lewis acidity values do not vary enough to ascertain this trend with certainty and reach a conclusion about the optimal values. The influence of Brønsted acidity seems, on the other hand, more evident. Hence, figure 10 shows a decrease in polymerization activity with the increase in Brønsted acidity. It is worth noting that Brønsted acidity is mainly weak in the case of DSAl supports, as seen in table 1, which indicates that polymerization activity may be inhibited by this type of acidity. This finding is in agreement with the work done by Campos *et al*[5].

Conclusions

A series of DSAl materials was prepared using recently reported and well-established procedures, which were used to develop supported zirconocene catalysts. The different synthesis procedures employed were found to have a small effect on morphology and contrarily, a significant effect on textural and surface acidity properties. Direct synthesis methods were found to favor materials with higher textural parameters and stronger acidity when compared to incipient wetness impregnation. Solid-state ^{27}Al-NMR and FT-IR spectroscopy results show the importance of the chemical environment of the aluminum species in the resulting acidic properties and its effect on catalytic performance. The present work shows that aluminum modified dendrimeric silica materials exhibit a unique behavior compared to other mesoporous silicas. Furthermore, the study corroborates the key role played by surface acidity on the zirconocene activation and catalytic performance in ethylene polymerization. It was shown that weak Brønsted acid sites inhibit polymerization activity while Lewis acid sites appear to

present an optimum range for catalytic performance enhancement. Nevertheless, other effects of different nature, such as changes in textural properties and/or associated internal diffusion resistances may contribute to the final polymerization behavior. Therefore, a very complex balance of several effects must be taken in account when searching for an optimal support composition.

Experimental Section

Materials For the synthesis of the mesoporous materials, tetraethyl orthosilicate (TEOS, 99%, Aldrich), aluminum sulfate hexadecahydrate (98%, Fluka) and aluminum nitrate nonahydrate (98.5%, Merck) were used as silicon and aluminum precursors. 1-hexadecylpyridinium bromide hydrate (CPB, 98%, Alfa Aesar), cyclohexane (99.4%, Chem-Labs) and 1-pentanol (99.4%, VWR) were used as template, solvent and co-solvent, respectively. Regarding the ethylene polymerization reactions, zirconocene dichloride (Cp_2ZrCl_2, $Cp=\eta^5$-C_5H_5, Aldrich) was used as metallocene catalyst and methylaluminoxane (PMAO-IP 7wt% in toluene, Akzo Nobel) was used as co-catalyst. Ethylene and nitrogen (Air Liquide) were purified through adsorption columns containing a mixture of 4A and 13X molecular sieves. Toluene (VWR) was dried by refluxing over metallic sodium under nitrogen and using benzophenone as an indicator. Other materials were used without further purification. All sensitive reactants and materials were handled under nitrogen using standard inert atmosphere techniques.

Purely siliceous DS synthesis The synthesis procedure is described in the literature[24]. CPB (3g, 0.0078 mol) and urea (1.8 g, 0.03 mol) are dissolved in deionized water (90 mL). Separately, pentanol (1.5 mL) and TEOS (7.5 g, 0.036 mol) are dissolved in cyclohexane (90 mL). The two solutions are stirred separately to ensure homogenization. The organic solution is added to the aqueous solution under vigorous stirring and the resulting mixture is stirred for 30 minutes at room temperature. The micro-emulsion formed is finally treated at 120ºC with MW radiation for 60 minutes in Teflon autoclave vessels (MARS-5 oven, 600 W maximum power). The DS material is separated by centrifugation and washed twice with a 1:1 water and acetone solution. The resulting material is air-dried for 24 hours and after calcined at 650 ºC under air for 8 hours.

One-step DSAl Synthesis The synthesis procedure followed the procedure described above for purely siliceous DS with the addition of the required amount of aluminium sulfate to the initial aqueous solution, aiming to achieve a Si/Al ratio of 20. The DSAl material is separated by centrifugation and washed once with acetone and a second time with a 1:1 water and acetone solution. The resulting material is air-dried for 48 hours and after calcined at 650 ºC under air for 16 hours. The final material is referred to as DSAl-1step-**W**, where **W** indicates the Si/Al ratio.

Two-step DSAl Synthesis The synthesis procedure is based on the literature [4]. The preparation of the micro-emulsion is the same as described for purely siliceous DS. However, after 15 minutes of crystallization time under MW (120ºC, 600 W), the pH of the reaction mixture is adjusted to approximately 3 using a 2M HCl solution added dropwise. Afterwards, 2mL of an aluminum sulfate solution with the appropriate concentration required for Si/Al ratios of 10 or 20 is added to the reaction mixture, under stirring. The reaction then proceeds at 120ºC under MW radiation for 30 additional minutes. The DSAl material is separated by centrifugation and washed twice with a 1:1 water and acetone solution, and then air-dried for 48 hours. Calcination is then performed at 650 ºC under air for 16 hours. The final materials are referred to as DSAl-2steps-**W**, where **W** retains the same meaning as indicated before.

Incipient Wetness Impregnation Method For the preparation of a sample with a Si/Al of 20, an aqueous $Al(NO_3)_3$ solution is prepared with 475 mg of $Al(NO_3)_3 \cdot 9H_2O$ to be added in 3.1 mL (determined empirically). The solution is added dropwise to 1.5 g of pure-silica calcined DS and mechanically dispersed. After adding 3.1 mL, the powder begins to look wet and the overall volume decreases. The wet powder is left to rest for a few hours and is afterward dried overnight at 100ºC. The resulting material is calcined at 550ºC under air for 8 hours. The sample is referred to as IWI-DSAl-**W**, where **W** once again retains the same meaning.

Characterization Textural properties were obtained using nitrogen sorption measurements at 77K using a Micromeritics ASAP 2010 equipment. Prior to the measurements, the samples were degassed at 300ºC for 3 hours. Morphology was assessed by TEM microscopy (Hitachi H8100 Transmission Electron Microscope). Brønsted and Lewis acid site quantification was carried out through FT-IR spectroscopy with pyridine as a probe molecule. Self-supported wafers were placed in an IR quartz cell and evacuated under secondary vacuum (10^{-6} Torr) at 300ºC for 2 hours before pyridine adsorption at 150ºC (equilibrium pressure ~ 1.5 Torr). Subsequent desorption of pyridine was carried out under secondary vacuum at 150ºC and 300ºC for 30 minutes. The IR spectra were recorded on a Thermo Nicolet Nexus 670 instrument (64 scans, 4 cm^{-1} resolution). The background spectrum, recorded under identical operating conditions, was automatically subtracted from each sample spectrum. For quantitative measurements, pyridine extinction molar coefficients from Emeis[37] were used. Chemical composition was determined by AAS for Si content and ICP-AES for Al content.

Support Pretreatment A batch of DS or DSAl was treated at 200ºC under primary vacuum for 90 minutes to remove the adsorbed water.

Catalyst Immobilization Approximately 150 mg of dry support were weighed and stored in a schlenk tube. Toluene was added with a ratio of 29 mL per gram of support. A homogeneous solution of zirconocene dichloride in toluene was

prepared and transferred onto the support suspension to achieve the desired ratio of 12 or 20 µmol/g for DS or DSAl supports, respectively. The catalyst and support were contacted for 16 hours and afterwards directly injected into the reactor.

Ethylene Polymerization The polymerization reactor consists of a 250 mL bottle for pressure reactions (Wilmad LabGlass LG-3921), with crown cap, gasket and magnetic stirrer. This reactor was placed in a water bath. Ethylene consumption rate was measured using two mass flow controllers (Hastings Instruments HFC-202 and Alicat Scientific 16 Series) and recorded in a personal computer with data acquisition hardware and software (a ComputerBoards CIO-DAS08/Jr-A0 interface card with Labtech DataLab software). Ethylene pressure was measured with a digital manometer (AirLiquide M2500) and also recorded.

The reactor was purged with vacuum/N_2 and loaded with enough toluene to match a total volume of 50 mL when the polymerization was started. Nitrogen was replaced by ethylene and the appropriate amount of MAO co-catalyst solution was injected into the reactor, to get an Al/Zr ratio of 1500. Finally, a suspension of the supported catalyst was vigorously stirred and the equivalent to 2 x10^{-6} mol of Zr was injected into the reactor by measuring an adequate volume of suspension. During the reaction the temperature, pressure and ethylene mass flow data can be monitored in real-time and automatically recorded. The ethylene mass flow was converted to ethylene consumption and polymerization activity calculated in $kg_{PE}/mol_{Zr}h$. The kinetic profiles correspond to ethylene consumption versus time, which after integration yields a value of average activity that was compared to the value obtained by considering the mass of recovered polymer. The reaction was stopped either at the end of 30 minutes or when the consumption of ethylene reaches approximately 2 grams, in order to avoid severe mass transfer limitations occurring after this point. After the reaction, possible solubilized polymer is precipitated over HCl acidified methanol, filtered and washed twice using methanol before drying. The supernatant or clarified liquid test was followed as described in the literature[5].

Acknowledgements

The authors gratefully acknowledge the funding of this work by Fundação para a Ciência e Tecnologia (FCT), CQE-FCT (UID/QUI/00100/2013), the FCT-CATSUS program and the PAUILF (Project TC 04/17). D.M.Cecílio's PhD scholarship (PD/BD/114580/2016), A. Fernandes' grant (SFRH/BPD/91397/2012) provided by FCT are gratefully acknowledged. The authors are grateful to Prof. João Rocha (CICECO, Aveiro, Portugal) for the NMR characterization of the materials, Dr. Timothy F.L. McKenna and Dr. Christophe Boisson from LCPP-C2P2, Lyon, France for their valuable input during the development of this work.

Keywords: acidity • dendrimeric silica • ethylene polymerization • metallocenes • supported catalysts

[1] S. Lee, K. Y. Choi, *Macromol. React. Eng.* **2017**, *11*, 1600027.
[2] J. M. Campos, J. P. Lourenço, H. Cramail, M. R. Ribeiro, *Prog. Polym. Sci.* **2012**, *37*, 1764–1804.
[3] M. Hartmann, W. Schwieger, *Chem. Soc. Rev.* **2016**, *45*, 3311–3312.
[4] Y. Choi, Y. S. Yun, H. Park, D. S. Park, D. Yun, J. Yi, *Chem. Commun. (Camb).* **2014**, *50*, 7652–5.
[5] J. M. Campos, J. P. Lourenço, A. Fernandes, A. M. Rego, M. R. Ribeiro, *J. Mol. Catal. A Chem.* **2009**, *310*, 1–8.
[6] J. M. Campos, J. P. Lourenço, A. Fernandes, M. R. Ribeiro, *Catal. Commun.* **2008**, *10*, 71–73.
[7] J. M. Campos, M. R. Ribeiro, J. P. Lourenço, A. Fernandes, *J. Mol. Catal. A Chem.* **2007**, *277*, 93–101.
[8] H. Kosslick, G. Lischke, B. Parlitz, W. Storek, R. Fricke, *Appl. Catal. A Gen.* **1999**, *184*, 49–60.
[9] H. Kosslick, G. Lischke, H. Landmesser, B. Parlitz, W. Storek, R. Fricke, *J. Catal.* **1998**, *176*, 102–114.
[10] H. Landmesser, H. Kosslick, U. Kurschner, R. Fricke, *J. Chem. Soc. Faraday Trans.* **1998**, *94*, 971–977.
[11] H. Kosslick, G. Lischke, G. Walther, W. Storek, A. Martin, R. Fricke, *Microporous Mater.* **1997**, *9*, 13–33.
[12] H. Kosslick, H. Landmesser, R. Fricke, *J. Chem. Soc. Faraday Trans.* **1997**, *93*, 1849–1854.
[13] A. Corma, *Chem. Rev.* **1997**, *97*, 2373–2420.
[14] X. S. Zhao, G. Q. (Max) Lu, G. J. Millar, *Ind. Eng. Chem. Res.* **1996**, *35*, 2075–2090.
[15] M. Horňáček, P. Hudec, A. Smiešková, *Chem. Pap.* **2009**, *63*, 689.
[16] T. Tayano, H. Uchino, T. Sagae, K. Yokomizo, K. Nakayama, S. Ohta, H. Nakano, M. Murata, *Macromol. React. Eng.* **2017**, *11*, 1600017.
[17] D. W. Jeong, D. S. Hong, H. Y. Cho, S. I. Woo, *J. Mol. Catal. A Chem.* **2003**, *206*, 205–211.
[18] V. N. Panchenko, I. G. Danilova, V. A. Zakharov, N. V Semikolenova, E. A. Paukshtis, *React. Kinet. Mech. Catal.* **2017**, *122*, 275–287.
[19] T. Sano, T. Niimi, T. Miyazaki, S. Tsubaki, Y. Oumi, T. Uozumi, *Catal. Letters* **2001**, *71*, 105–110.
[20] A. Carrero, R. Van Grieken, I. Suarez, B. Paredes, *Polym. Eng. Sci.* **2008**, *48*, 606–616.
[21] T. Miyazaki, Y. Oumi, T. Uozumi, H. Nakajima, S. Hosoda, T. Sano, *Stud. Surf. Sci. Catal.* **2002**, *142*, 871–878.
[22] T. Sano, Y. Oumi, *Catal. Surv. from Asia* **2004**, *8*, 295–304.
[23] H. Rahiala, I. Beurroies, T. Eklund, K. Hakala, R. Gougeon, P. Trens, J. B. Rosenholm, *J. Catal.* **1999**, *188*, 14–23.
[24] V. Polshettiwar, D. Cha, X. Zhang, J. M. Basset, *Angew. Chemie - Int. Ed.* **2010**, *49*, 9652–9656.
[25] N. Bayal, B. Singh, R. Singh, V. Polshettiwar, *Sci. Rep.* **2016**, *6*, 24888.
[26] L. Ernawati, R. Balgis, T. Ogi, K. Okuyama, *Langmuir* **2016**, *33*, 783–790.
[27] J. Yang, D. Shen, Y. Wei, W. Li, F. Zhang, B. Kong, S. Zhang, W. Teng, J. Fan, W. Zhang, et al., *Nano Res.* **2015**, *8*, 2503–2514.
[28] F. Shahangi, A. Najafi Chermahini, M. Saraji, *J. Energy Chem.* **2017**, DOI https://doi.org/10.1016/j.jechem.2017.06.004.

[29] S. Afzal, X. Quan, S. Chen, J. Wang, D. Muhammad, *J. Hazard. Mater.* **2016**, *318*, 308–318.

[30] M. M. Stalzer, M. Delferro, T. J. Marks, *Catal. Letters* **2015**, *145*, 3–14.

[31] M. Jezequel, V. Dufaud, M. J. Ruiz-Garcia, F. Carrillo-Hermosilla, U. Neugebauer, G. P. Niccolai, F. Lefebvre, F. Bayard, J. Corker, S. Fiddy, et al., *J. Am. Chem. Soc.* **2001**, *123*, 3520–3540.

[32] C. P. Nicholas, H. Ahn, T. J. Marks, *J. Am. Chem. Soc.* **2003**, *125*, 4325–4331.

[33] T. J. Marks, *Acc. Chem. Res.* **1992**, *25*, 57–65.

[34] C. Christophe, C. Mathieu, P. S. Romain, B. Jean-Marie, *Angew. Chemie Int. Ed.* **2003**, *42*, 156–181.

[35] N. Millot, S. Soignier, C. C. Santini, A. Baudouin, J.-M. Basset, *J. Am. Chem. Soc.* **2006**, *128*, 9361–9370.

[36] J. M. Campos, Polimerização de Etileno Com Zirconoceno Suportado Em MCM-41 Modificado: Estudo Catalítico e Propriedades Dos Materiais Obtidos, PhD Thesis, UTL, Instituto Superior Técnico, **2009**.

[37] C. A. Emeis, *J. Catal.* **1993**, *141*, 347–354.

Entry for the Table of Contents (Please choose one layout)

Layout 1:

FULL PAPER

Acidity and textural features. Do they matter? Acidity has a critical role in the ethylene polymerization activity of zirconocene dichloride supported on Al-containing dendrimeric silica nanospheres. However, the textural properties of the non-conventional porous structure supports should not be neglected

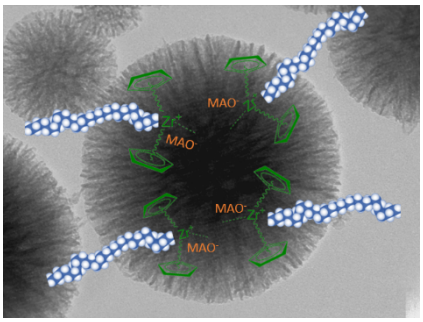

Duarte M. Cecílio, Auguste Fernandes, João Paulo Lourenço and M. Rosário Ribeiro**

Page No. – Page No.

Aluminum containing dendrimeric silica nanoparticles as promising metallocene catalyst supports for ethylene polymerization

Layout 2:

FULL PAPER

((Insert TOC Graphic here; max. width: 11.5 cm; max. height: 2.5 cm))

*Author(s), Corresponding Author(s)**

Page No. – Page No.

Title

Text for Table of Contents